

A simplified framework for fast and reliable measurement of leaf turgor loss point

Francesco Petruzzellis^{1*}, Tadeja Savi², Giovanni Bacaro¹, Andrea Nardini¹

¹Dipartimento di Scienze della Vita, Università degli Studi di Trieste, via L. Giorgieri 10, 34127, Trieste, Italia

²University of Natural Resources and Life Sciences, Vienna, Department of Crop Sciences, Division of Viticulture and Pomology, Konrad Lorenz Straße 24, A-3430 Tulln, Austria

*Corresponding author: fpetruzzellis@units.it

HIGHLIGHTS:

- Leaf turgor loss point (Ψ_{tlp}) defines drought tolerance of plant species.
- Ψ_{tlp} could be estimated from the osmotic potential at full turgor (π_0).
- π_0 could be easily measured with a dewpoint hygrometer.
- Accounting for leaf dry matter content improves estimates of Ψ_{tlp} from π_0 .

22 ABSTRACT:

23 Drought tolerance shapes the distribution of plant species, and it is mainly
24 determined by the osmotic potential at full turgor (π_0) and the water potential at turgor
25 loss point (Ψ_{tlp}). We provide a simplified framework for π_0 and Ψ_{tlp} measurements
26 based on osmometer determination of π_0 (π_{0_osm}). Specifically, we ran regression
27 models to i) improve the predictive power of the estimation of π_0 from π_{0_osm} and
28 morpho-anatomical traits; ii) obtain the most accurate model to predict Ψ_{tlp} on the
29 basis of the global relationship between π_0 and Ψ_{tlp} . The inclusion of the leaf dry
30 matter content (LDMC), an easy-to-measure trait, in the regression model improved
31 the predictive power of the estimation of π_0 from π_{0_osm} . When π_{0_osm} was used as a
32 simple predictor of Ψ_{tlp} , discrepancies arose in comparison with global relationship
33 between π_0 and Ψ_{tlp} . Ψ_{tlp} values calculated as a function of the π_0 derived from π_{0_osm}
34 and LDMC (π_{0_fit}) were consistent with the global relationship between π_0 and Ψ_{tlp} .
35 The simplified framework provided here could encourage the inclusion of
36 mechanistically sound drought tolerance traits in ecological studies.

38 KEYWORDS:

39 dewpoint hygrometer; mechanistic traits; osmotic potential; water availability; water
40 potential

1. INTRODUCTION

Plant functional traits are defined as morphological, physiological, or phenological features measurable at the individual level, from the cell to the whole-organism (Violle et al., 2007). Recently, Brodribb (2017) suggested to distinguish “mechanistic” traits, which comprehends plant’s features clearly associated to a physiological process, from general functional traits (such as leaf mass per unit area), which rather represent “syndromes” that could be driven by several different physiological functions and associated trade-offs. Mechanistic traits have been increasingly included in trait-based studies and provided novel insights into several ecological processes, ranging from species assembly rules (Blackman et al., 2012; Brodribb et al., 2014), invasion of alien plant species (Petrussellis et al., 2018), and vegetation dynamics under ongoing climate changes (Anderegg, 2015). As an example, hydraulic traits (e.g. Ψ_{50} , the water potential inducing 50% loss of hydraulic conductivity, or K_s , the stem specific hydraulic conductivity) have been used to model plant species distribution (Costa-Saura et al., 2016; Larter et al., 2017), and they were shown to correlate with growth rate and risk of mortality under drought (Anderegg et al., 2015; Choat et al., 2012; Fan et al., 2012).

Leaf water relation parameters have been recently proposed as predictors of the position of a species along the “fast-slow” whole plant economic spectrum (Blackman, 2018; Zhu et al., 2018), as they correlate to both leaf hydraulic and economic traits (Nardini and Luglio, 2014; Trifiló et al., 2016). Specifically, leaf osmotic potential at full turgor (π_0) and the leaf water potential at turgor loss point (Ψ_{tlp}) are strongly linked to species-specific ability to tolerate leaf dehydration (Bartlett et al., 2012b) and consequently to sustain stomatal conductance, photosynthesis and growth even under water shortage conditions (Bartlett et al., 2016; Tognetti et al., 2000). In particular, Ψ_{tlp} indicates the water potential inducing loss of cell turgor pressure (Bartlett et al., 2012b), which is critical to maintain gas exchange and growth (Brodribb et al. 2003). In their recent analysis, Zhu et al. (2018) have reported that Ψ_{tlp} is correlated with leaf carbon investment, as species with lower Ψ_{tlp} tend to have higher leaf density (d_{leaf}) and leaf mass per unit area (LMA). Turgor loss point also correlates with habitat moisture, as species living in arid environments usually have lower values of Ψ_{tlp} than species living under higher water availability (Bartlett et al., 2012b; Lenz et al., 2006; Zhu et al., 2018). Given the correlation between Ψ_{tlp} ,

hydraulic and economic traits and environmental features, the inclusion of the turgor loss point in ecological studies holds promises to provide important insights on ecological and evolutionary patterns in plants.

Ψ_{tlp} has been traditionally estimated from water potential isotherms (or pv-curves, Tyree and Hammel 1972), i.e. by measuring the progressive decrease of the water potential and of the water content during leaf dehydration. This procedure is time-consuming, and this probably limited the inclusion of Ψ_{tlp} in studies involving large numbers of species/individuals and/or study sites. Recently, Bartlett et al. (2012b) have reported that the variation of Ψ_{tlp} both between and within species is mainly driven by changes in π_0 , which reflects solutes concentration in cells at full turgor. These two traits resulted highly correlated to each other, as species with lower Ψ_{tlp} also have lower values of π_0 (Bartlett et al., 2012b). Consequently, both traits could be considered as useful parameters to predict species drought tolerance, and π_0 could be used as a proxy of turgor loss point. Alternative methods have been proposed to obtain π_0 , e.g. by directly measuring the osmotic potential of sap extracted from leaf tissues using a thermocouple psychrometer. In particular, rapid freeze and thaw of leaf samples, that induces cell disruption and the release of symplastic contents, is considered the most accurate procedure to measure π_0 with an osmometer (π_{0_osm}). Recently, Bartlett et al. (2012a) proposed a framework to predict both π_{0_pv} (osmotic potential at full turgor derived from pv-curves) and Ψ_{tlp} from π_{0_osm} measurements. In their analysis, the authors tested various models including different morpho-anatomical leaf traits, and they reported that models including bulk modulus of elasticity (ϵ) and d_{leaf} significantly improved the ability to predict π_{0_pv} from π_{0_osm} measurements. However, ϵ is generally derived from pv-curves, so that including this parameter in the derivation of π_{0_pv} does not represent a major advantage. Also, d_{leaf} measurements can be laborious and prone to errors as far as volume estimates are concerned. Hence, a simplified framework for estimation of π_0 would be useful for ecological studies.

In this study, we measured several functional traits as well as water relation parameters derived from pv-curves in 27 species, with the aim to provide a simple framework to estimate π_{0_pv} and Ψ_{tlp} from measurements of π_{0_osm} obtained with a dewpoint hygrometer. The specific aims were to i) obtain a model to predict π_{0_pv} on the basis of π_{0_osm} and easy-to-measure functional traits (like LMA or leaf dry matter

content); ii) obtain the most accurate model to predict Ψ_{tlp} on the basis of the global relationship between π_0 and Ψ_{tlp} .

2. MATERIALS AND METHODS

2.1 Leaf traits measurements

To model the estimation of the osmotic potential at full turgor (π_0) and of the water potential at turgor loss point (Ψ_{tlp}) from π_0 values obtained with a dewpoint hygrometer (π_{0_osm} ; see below), we selected 27 temperate and Mediterranean woody species (Table S1) with different levels of drought resistance. Species were sampled in natural habitats in the Karst region (NE Italy), or in the Botanical Garden of University of Trieste. Additional data were obtained from previous studies performed in our laboratory (see Table S1 for references).

Three leaves were sampled from different individuals of each species to measure π_{0_osm} . Twigs were detached from branches and were rehydrated overnight. One leaf per twig was roughly crumpled up and sealed in cling film. Then, it was immersed in liquid nitrogen (LN_2) for 2 min. The leaf (still sealed in cling film) was then carefully ground and stored in sealed plastic bottles at -20°C . Before measurements, samples were thawed at room temperature for 5 min while still sealed in cling film and in plastic bottles, to avoid evaporation effect on measurements (Bartlett et al., 2012a). Finally, π_{0_osm} was measured with a dewpoint hygrometer (Model WP4, Decagon Devices Inc., Pullman, Washington, USA).

Water potential isotherms (pv-curves) were measured to obtain reference values for Ψ_{tlp} and π_{0_pv} . Fresh leaves were rehydrated for 12 h with their petioles immersed in pure water and pv-curves were measured using the bench dehydration technique, by repeatedly measuring water loss and water potential with a balance and a pressure chamber (model 1505D, PMS Instruments, Albany, OR, USA), respectively, during progressive sample dehydration. Water potential (Ψ_{leaf}) and cumulative weight loss (WI) of leaves were measured until the relationship between $1/\Psi$ and WI became strictly linear, indicating the loss of cell turgor. Pv-curves were then elaborated according to Salleo (1983) to calculate the osmotic potential at full turgor (π_{0_pv}), the water potential at turgor loss point ($\Psi_{\text{tlp_pv}}$) and the modulus of elasticity (ϵ).

For each species, leaf morpho-anatomical parameters were measured on 6 leaves from the same individuals sampled for the measurements of π_{0_osm} and pv-curves. Specifically, we measured leaf thickness (Th, μm), leaf dry matter content (LDMC, mg g^{-1}), leaf mass per unit area (LMA, mg cm^{-2}) and leaf density (d_{leaf} , g cm^{-3}).

Th was measured after rehydrating leaves for 3h using a digital calliper on three portions of the leaf (top, middle, bottom). Values were then averaged for each leaf.

LDMC and LMA were calculated as:

$$\text{LDMC} = \text{Leaf dry weight} / \text{Leaf turgid weight} \quad (\text{eqn 1})$$

$$\text{LMA} = \text{Leaf dry weight} / \text{Leaf area} \quad (\text{eqn 2})$$

Fresh leaves were first rehydrated for 3h and leaf turgid weight was measured with an analytical balance. Leaves were scanned and leaf area was measured using the software Image J (Schneider et al., 2012). Leaves were finally oven-dried for 48 h at 72°C and leaf dry weight was measured.

d_{leaf} was calculated as:

$$d_{\text{leaf}} = \text{Leaf dry weight} / \text{Leaf fresh volume} \quad (\text{eqn 3})$$

Leaf fresh volume was measured using a water displacement method (Hughes 2005), while leaf dry weight was measured as described above.

2.2 Statistical analysis

The first aim of this study was to find an easy and fast method to measure the leaf osmotic potential at full turgor, based on the work of Bartlett et al. (2012a). To improve the predictive power of the estimation of π_{0_pv} from π_{0_osm} measurements, we ran a multiple linear regression model to predict π_{0_pv} (response variable) as a function of π_{0_osm} and the leaf traits described above. A Minimum Adequate Model (MAM) was obtained using package “glmulti” (Calcagno 2013) via minimization of the corrected Akaike informative criterion (AICc) plus a backward procedure to avoid multicollinearity among selected explanatory variables. To compare results obtained by Bartlett et al. (2012a), we evaluated two other linear regression models, setting π_{0_pv} as the response variable. In a first model, only π_{0_osm} was set as the predictive variable, while in the second we considered both π_{0_osm} and d_{leaf} as predictive variables. Models were then compared on the basis of their predictive power

(adjusted R^2 , R^2_{adj}) and, in order to take in account the number of predictors included in the model, the AICc and their mean absolute error (MAE).

The second aim of this study was to test the ability to predict Ψ_{tlp_pv} both from π_{0_osm} measurements and the fitted values of the MAM (π_{0_fit}) and compare models' output with the global relationship between Ψ_{tlp} and π_0 described in Bartlett et al. (2012b). We first fitted two separated simple linear regression models on the data measured in the present study, considering Ψ_{tlp_pv} (response variable) as a function of π_{0_osm} or π_{0_fit} , respectively. For each model, we calculated coefficient estimates and associated 95% confidence intervals (95% C.I.), R^2_{adj} , AICc and MAE.

Because the number of species analysed in Bartlett et al. (2012b) differed from the present study (248 and 27 respectively), we set up a bootstrap procedure (999 replicates) to obtain comparable values of estimated coefficients. π_0 and Ψ_{tlp} values of 27 randomly selected species from the dataset in Bartlett et al. (2012b) were chosen. From this selection, we fitted a simple linear regression model calculating coefficient estimates, 95% C.I., R^2_{adj} , AICc and MAE. At the end of this bootstrap procedure, averaged values were calculated. Differences between Ψ_{tlp_pv} prediction from π_{0_osm} , π_{0_fit} and the one derived from Bartlett et al. (2012b) were determined comparing 95% C.I. of the coefficient estimates and AICc. Specifically, predictions were assumed to differ if 95% C.I. of coefficient estimates did not overlap and if the difference between AICc values were > 2 (Burnham and Anderson, 2004). All statistical analyses were performed using R 3.4.1 (R Foundation for Statistical Computing, Vienna, AT).

3. RESULTS

Species scientific name, abbreviation, and associated mean values of leaf traits are summarized in Tab. S1. Species that sustained higher leaf construction costs (higher LMA, LDMC and Th) also had higher drought resistance (lower Ψ_{tlp_pv}), as shown by correlation analysis reported in Tab. S2.

Although π_{0_osm} resulted a significant predictor π_{0_pv} (Tab. 1), it underestimated π_{0_pv} at less negative values and overestimated it at more negative values (Fig. 1). The best model to predict π_{0_pv} included π_{0_osm} and LDMC as predictive variables (Tab. 1). The inclusion of LDMC significantly improved the

predictive power of the model, as the R^2_{adj} was higher and AICc were lower than those calculated on the model including only π_{0_osm} or the one including both π_{0_osm} and ϵ (Tab. 1).

Tab. 1 Summary of the models predicting the osmotic potential at full turgor measured through pv-curves (π_{0_pv}) from osmotic potential at full turgor obtained with a dewpoint hygrometer (π_{0_osm}) alone, including leaf dry matter content (LDMC) or the modulus of elasticity of cell walls (ϵ). R^2_{adj} = adjusted r^2 . AICc = Akaike informative criterion corrected for low number of observations. MAE = mean absolute error of the model

π_{0_PV} estimation	Estimate	Std. error	p-value	R^2_{adj}	AICc	MAE
$\beta * \pi_{0_osm} + \text{intercept}$				0.46	17.8	0.18
β	0.681	0.143	<0.001			
intercept	-0.434	0.240	0.08			
$\beta * \pi_{0_osm} + \beta_1 * \text{LDMC} + \text{intercept}$				0.58	11.4	0.12
β	0.506	0.138	0.001			
β_1	-0.002	0.001	0.007			
intercept	0.013	0.258	0.96			
$\beta * \pi_{0_osm} + \beta_1 * \epsilon + \text{intercept}$				0.53	16.1	0.17
β	0.654	0.226	0.17			
β_1	-0.013	0.132	<0.001			
intercept	-0.319	0.006	0.03			

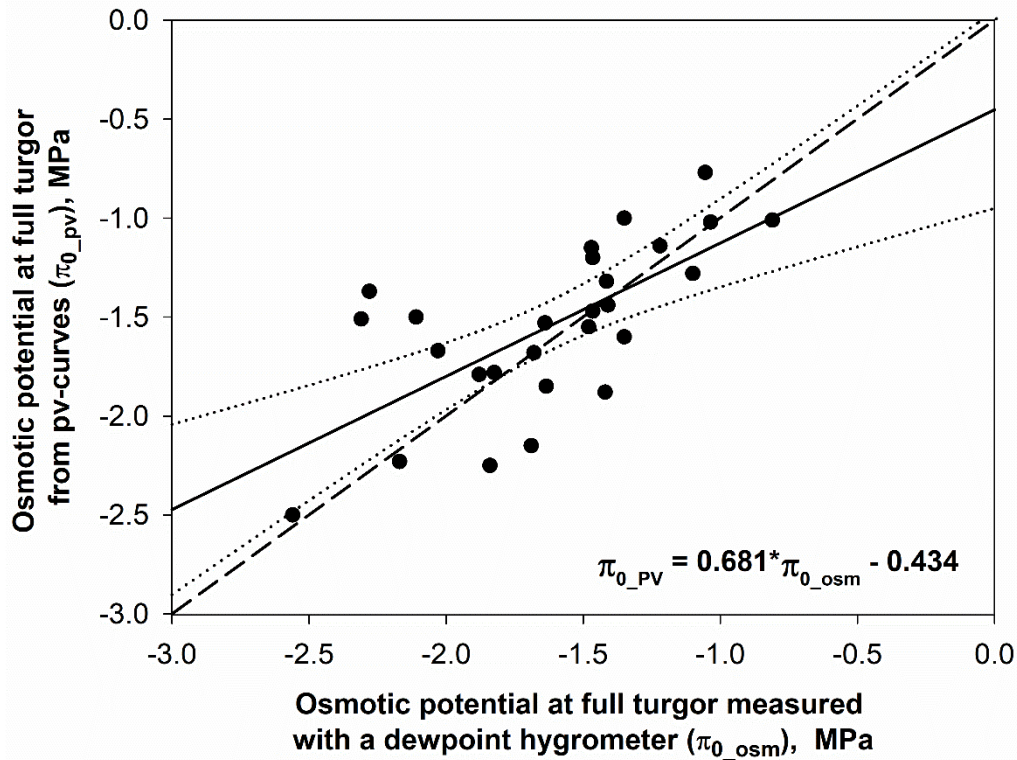


Fig. 1 Relationship between osmotic potential at full turgor measured with a dewpoint hygrometer (π_{0_osm}) and osmotic potential at full turgor measured through pv-curves (π_{0_pv}). Dotted lines represent confidence intervals of the regression line (solid line). Dashed line represents the 1:1 line

π_{0_osm} and π_{0_fit} were tested as predictors of Ψ_{tlp_pv} . The parameters of the two derived models were compared with those derived from the relationship between Ψ_{tlp_pv} and π_{0_pv} reported in Bartlett et al. (2012b) and from the iterative procedure described above. The average β and intercept estimates calculated on a reduced number of species were not statistically different from those calculated including the whole dataset provided by Bartlett et al. (2012b) and on the models including π_{0_osm} and π_{0_fit} as predictive variables, as 95% C.I. overlapped each other (Tab. 2). However, the model including π_{0_fit} had higher predictive ability than the one including π_{0_osm} (Tab.1), as the R^2_{adj} was higher and AICc and MAE were lower (Tab. 2). In addition, the model including π_{0_osm} led to overestimation of Ψ_{tlp_pv} for values < -2 MPa. As shown in Fig. 2 and Fig. 3, mean values of slope (β) and intercept

calculated on the model including π_{0_fit} as predictive variable were much closer to those calculated on 27 randomly selected species from Bartlett et al. (2012b).

Tab. 2 Summary of the models predicting the water potential at turgor loss point measured through pv-curves (Ψ_{tlp_pv}) from osmotic potential at full turgor obtained with a dewpoint hygrometer (π_{0_osm}) alone, fitted values of the MAM (π_{0_fit}) and from π_0 values provided by Bartlett et al. (2012b). 2.5% and 97.5% represent 95% confidence interval limits. R^2_{adj} = adjusted R^2 . AICc = Akaike informative criterion corrected for low number of observations. MAE = mean absolute error of the model.

Ψ_{tlp_pv} estimation	Estimate	2.5%.	97.5%	R^2_{adj}	AICc	MAE
$\beta * \pi_{0_osm} + \text{intercept}$				0.47	31.4	0.31
β	0.899	0.530	1.268			
intercept	-0.581	-1.197	0.034			
$\beta * \pi_{0_fit} + \text{intercept}$				0.61	23.9	0.25
β	1.313	0.902	1.725			
intercept	-0.032	-0.673	0.609			
$\beta * \pi_{0_pv} + \text{intercept}$ (27 species)				0.87	6.82	0.18
β	1.211	1.027	1.394			
intercept	-0.057	-0.391	0.276			
$\beta * \pi_{0_pv} + \text{intercept}$ (Bartlett et al., 2012b)				0.87	50.1	0.18
β	1.205	1.146	1.263			
intercept	-0.062	-0.170	0.044			

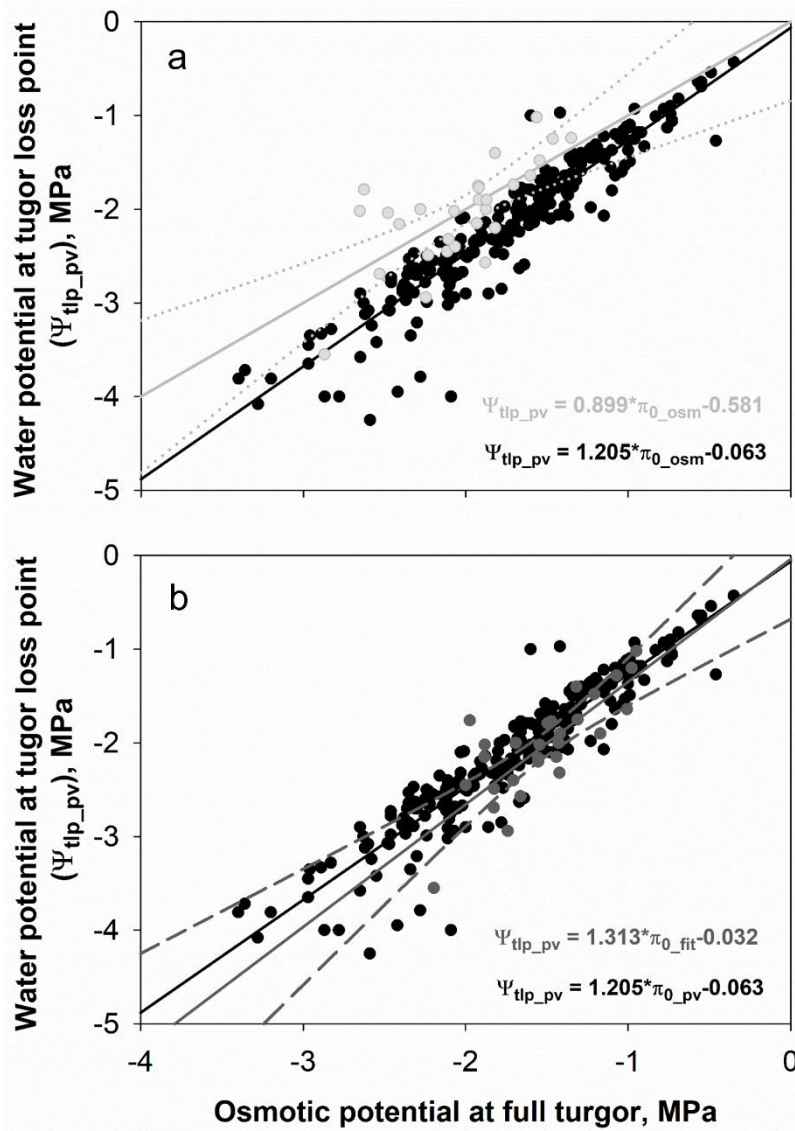


Fig. 2 Relationship between water potential at turgor loss point measured through pv-curves (Ψ_{tlp_pv}) and the osmotic potential at full turgor measured with a dewpoint hygrometer (π_{0_osc} , light grey circles, a), the fitted values of the MAM (π_{0_fit} , dark grey circles, b) and the osmotic potential at full turgor from Bartlett et al. (2012b, black circles). Dotted light green line represents confidence intervals of the regression line calculated considering π_{0_osc} (solid light grey line, a). Dashed dark grey line represents confidence intervals of the regression line calculated considering π_{0_fit} (solid dark grey line, b). Solid black lines represent regression lines calculated on data from Bartlett et al. (2012b).

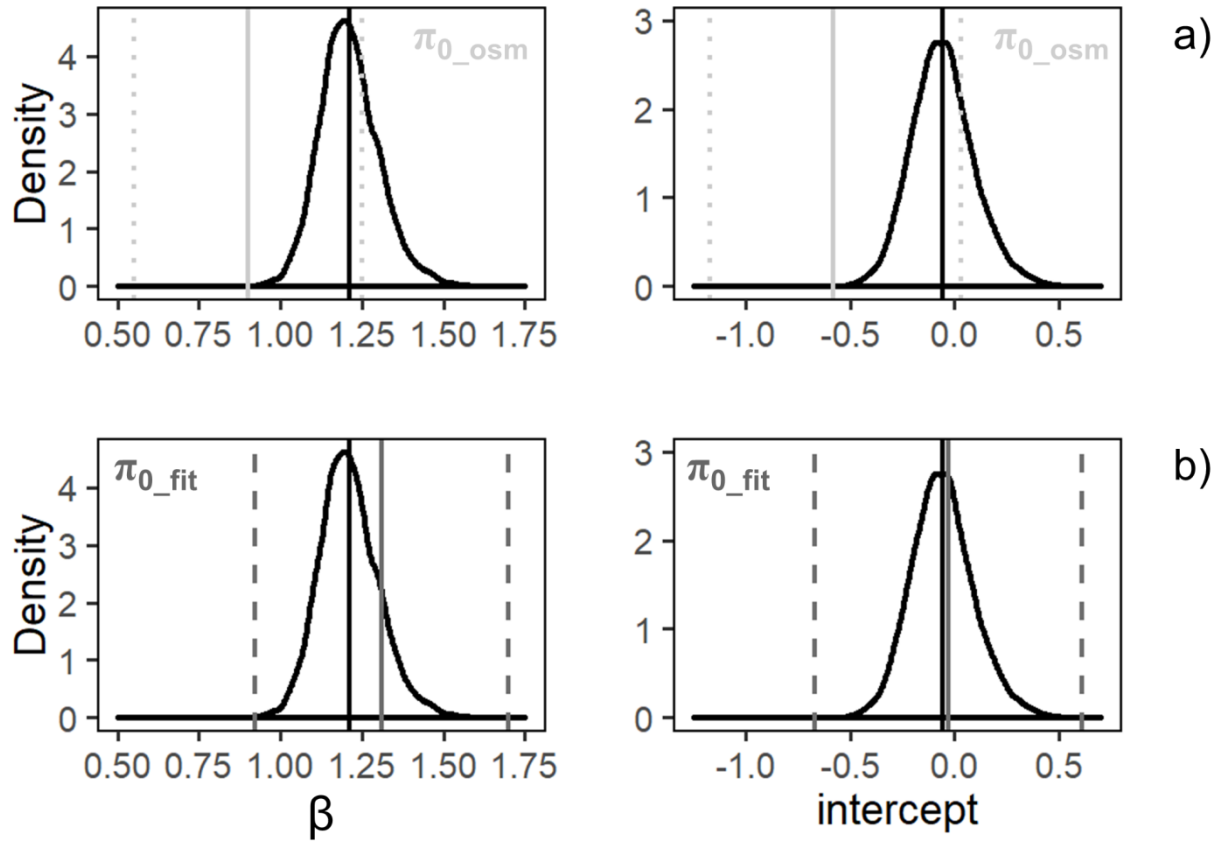


Fig. 3 Density probability and associated mean values (black solid lines) of coefficient β and intercept of the model predicting Ψ_{tlp_pv} calculated on a reduced subset of data from Bartlett et al. (2012b). Solid and dotted light grey lines represent mean values and 95% C.I. of coefficient β and intercept calculated on the model including π_{0_osm} as predictive variable (a). Solid and dashed dark grey lines represent mean values and 95% C.I. of coefficient β and intercept calculated on the model including π_{0_fit} as predictive variable (b).

4. DISCUSSION

As reported by Bartlett et al. (2012a), π_{0_osm} significantly correlated with π_{0_pv} (Fig. 1), but the regression line was different from the desired 1:1 relationship. A reason for this discrepancy is that osmometer-based measurements of π_0 could be biased by errors due to sample preparation. In fact, the disruption of cell walls could cause the dissolution of cell walls solutes that could lead to more negative π_0 values. On the other hand, symplastic fluids could be diluted by apoplastic water, leading to higher π_0 values. In this light, testing whether this prediction could be improved is fundamental to provide a solid framework for fast and reliable π_0 estimation. In the present study, we measured several leaf morpho-anatomical traits in order to enhance the predictive power of π_{0_pv} from measurements done with an hygrometer (π_{0_osm}) on the basis of the framework proposed by Bartlett et al. (2012a).

The best model to predict π_{0_pv} included π_{0_osm} and LDMC, enhancing the predictive power of the model including only π_{0_osm} , as R^2_{adj} was higher and AICc and MAE were lower (Tab. 1). As previously suggested by Bartlett et al. (2012a), the inclusion of LDMC in the predictive model could account for both errors associated to osmometer measurements. Higher values of LDMC are associated to greater cell wall investment, which in turn could improve the maintenance of relatively high water content, thus accounting for apoplastic dilution. On the other hand, higher LDMC could also reflect thicker cell walls or leaf with smaller but more numerous cells, thus accounting for solutes concentration enrichment derived from cell walls disruption.

In their analysis, Bartlett et al. (2012a) found that the best models to predict π_{0_pv} included d_{leaf} , π_{0_osm} and their interaction, or just ϵ and π_{0_osm} . In our analysis, d_{leaf} was discarded during model selection and the model including ϵ had less predictive power than the model including LDMC. These discrepancies could be due to multiple factors. Both studies included a limited number of species (30 in Bartlett et al. (2012a) and 27 in the present study), adapted to different environments. Most of the species in the present study are typical of Mediterranean biomes, while most of the species in Bartlett et al. (2012a) originate from temperate and tropical biomes. Consequently, drought tolerance and turgor loss point could be driven by different morpho-anatomical features in the two sets of species. Moreover, whereas minimum and maximum π_{0_pv} values were nearly the same between the two datasets, the distribution of density probability of π_0 was more skewed in Bartlett et al. (2012a)

(Fig. S1), indicating a higher density of observations in a narrower range of π_0 values. However, a sort of consensus approach could be derived from these analyses. In both studies, the best model to predict π_{0_pv} included traits which reflect leaf carbon investment (d_{leaf} , LDMC and ϵ), suggesting that species that sustain higher leaf construction costs (denser and/or thicker leaves), and thus occupy the “slow-growing” space of leaf economic spectrum (Wright et al., 2004), also have higher drought resistance. The framework provided by Bartlett et al. (2012a) could allow to estimate π_0 and Ψ_{tlp} on a large number of species and samples strongly reducing the time needed for its measurement using pv-curves. The framework provided in this study further simplifies the model proposed by Bartlett et al. (2012a), as the measurement of LDMC is faster and simpler than the procedure for d_{leaf} measurement.

π_0 and Ψ_{tlp} are strongly correlated with each other (Bartlett et al., 2012b) and thus, it is possible to estimate Ψ_{tlp} from measurements of π_0 . A significant linear relationship between π_0 and Ψ_{tlp} was found in the regression models run on the data provided by the authors (Tab. 2). We used parameters estimates of this model as a reference to compare regression models with π_{0_osm} or π_{0_fit} as predictive variable. The model including π_{0_osm} resulted very similar to the one obtained by Bartlett et al. (2012a):

$$\Psi_{tlp_pv} = 0.832 \pi_{0_osm} - 0.631 \quad (\text{eqn 4, from Bartlett et al. 2012a})$$

$$\Psi_{tlp_pv} = 0.899 \pi_{0_osm} - 0.581 \quad (\text{eqn 5})$$

However, the regression model in eqn 5 had a lower predictive power and parameters' estimates were slightly different than those calculated from the model run on data from Bartlett et al. (2012b) (Tab. 2). As shown in Fig. 2, we detected a discrepancy between the regression model considering π_{0_osm} as the predictive variable and the one calculated on data from Bartlett et al. (2012b). In particular, Ψ_{tlp} values < -2 MPa tended to be overestimated by eqn 2. On the contrary, the model considering π_{0_fit} as explanatory variable produced parameters' estimates much closer to those obtained from data provided in Bartlett et al. (2012b) (Fig. 2) and no discrepancy was detected.

The number of studies including π_0 and Ψ_{tlp} estimation from osmometer/hygrometer measurement of π_0 rapidly increased in the last years (Maréchaux et al., 2015; Petruzzellis et al., 2018, 2017), and it is likely that the

number of species with associated Ψ_{tlp} values will increase as well. In this light, the standardization and the simplification of the framework for Ψ_{tlp} estimation is crucial to build a solid global dataset. To improve the predictive power of the estimation of Ψ_{tlp} , we suggest measuring LDMC as well as π_{0_osm} from leaves attached to the same twig or at least belonging to the same individual. To estimate π_0 and Ψ_{tlp} we then suggest applying the following equations:

$$\pi_{0_fit} = 0.506\pi_{0_osm} - 0.002LDMC \text{ (expressed in mg g}^{-1}\text{)} \quad (\text{eqn 6})$$

$$\Psi_{\text{tlp_pv}} = 1.313\pi_{0_fit} - 0.032 \quad (\text{eqn 7})$$

Clearly, the inclusion of more species and π_0 values in this type of analysis is needed to furtherly optimize the framework for Ψ_{tlp} estimation.

CONTRIBUTIONS:

FP, TS and AN conceived and designed the study; FP and TS collected the data; FP, GB and AN analysed the data; FP, GB and AN wrote the manuscript, with the contribution of all authors.

FUNDING:

This work is part of the project 'Functional traits as a tool to predict invasive potential by alien species in different native communities', funded by University of Trieste (Finanziamenti per la Ricerca di Ateneo 2015).

ACKNOWLEDGMENTS:

We thank Roberto Alberti for help in collecting samples and Enrico Tordini for helpful comments during data analysis.

CONFLICT OF INTEREST:

The authors claim no conflict of interest.

REFERENCES

- Anderegg, W.R.L., 2015. Spatial and temporal variation in plant hydraulic traits and their relevance for climate change impacts on vegetation. *New Phytol.* 205, 1008–1014.
- Anderegg, W.R.L., Flint, A., Huang, C., Flint, L., Berry, J.A., Davis, F.W., Sperry, J.S., Field, C.B., 2015. Tree mortality predicted from drought-induced vascular damage. *Nat. Geosci.* 8, 367–371.
- Bartlett, M.K., Klein, T., Jansen, S., Choat, B., Sack, L., 2016. The correlations and sequence of plant stomatal, hydraulic, and wilting responses to drought. *P. Natl. A. Sci.* 113, 13098–13103.
- Bartlett, M.K., Scoffoni, C., Ardy, R., Zhang, Y., Sun, S., Cao, K., Sack, L., 2012a. Rapid determination of comparative drought tolerance traits: using an osmometer to predict turgor loss point: *Rapid assessment of leaf drought tolerance*. *Methods Ecol. Evol.* 3, 880–888.
- Bartlett, M.K., Scoffoni, C., Sack, L., 2012b. The determinants of leaf turgor loss point and prediction of drought tolerance of species and biomes: a global meta-analysis. *Ecol. Lett.* 15, 393–405.
- Blackman, C.J., 2018. Leaf turgor loss as a predictor of plant drought response strategies. *Tree Physiol.* 38, 655–657.
- Blackman, C.J., Brodribb, T.J., Jordan, G.J., 2012. Leaf hydraulic vulnerability influences species' bioclimatic limits in a diverse group of woody angiosperms. *Oecologia* 168, 1–10.
- Brodribb, T.J., 2017. Progressing from 'functional' to mechanistic traits. *New Phytol.* 215, 9–11.
- Brodribb, T.J., Holbrook, N.M., Edwards, E.J., Gutierrez, M.V., 2003. Relations between stomatal closure, leaf turgor and xylem vulnerability in eight tropical dry forest trees. *Plant Cell Environ.* 26, 443–450.
- Brodribb, T.J., McAdam, S.A.M., Jordan, G.J., Martins, S.C.V., 2014. Conifer species adapt to low-rainfall climates by following one of two divergent pathways. *P. Natl. A. Sci.* 111, 14489–14493.
- Calcagno, V., 2013. glmulti: Model selection and multimodel inference made easy. R package version 1.0.7.

- Choat, B., Jansen, S., Brodribb, T.J., Cochard, H., Delzon, S., Bhaskar, R., Bucci, S.J., Feild, T.S., Gleason, S.M., Hacke, U.G., Jacobsen, A.L., Lens, F., Maherali, H., Martínez-Vilalta, J., Mayr, S., Mencuccini, M., Mitchell, P.J., Nardini, A., Pittermann, J., Pratt, R.B., Sperry, J.S., Westoby, M., Wright, I.J., Zanne, A.E., 2012. Global convergence in the vulnerability of forests to drought. *Nature* 491, 752–755.
- Costa-Saura, J.M., Martínez-Vilalta, J., Trabucco, A., Spano, D., Mereu, S., 2016. Specific leaf area and hydraulic traits explain niche segregation along an aridity gradient in Mediterranean woody species. *Perspect. Plant Ecol.* 21, 23–30.
- Fan, Z.-X., Zhang, S.-B., Hao, G.-Y., Ferry Slik, J.W., Cao, K.-F., 2012. Hydraulic conductivity traits predict growth rates and adult stature of 40 Asian tropical tree species better than wood density. *J. Ecol.* 100, 732–741.
- Larter, M., Pfautsch, S., Domec, J.-C., Trueba, S., Nagalingum, N., Delzon, S., 2017. Aridity drove the evolution of extreme embolism resistance and the radiation of conifer genus *Callitris*. *New Phytol.* 215, 97–112.
- Lenz, T.I., Wright, I.J., Westoby, M., 2006. Interrelations among pressure-volume curve traits across species and water availability gradients. *Physiol. Plantarum* 127, 423–433.
- Maréchaux, I., Bartlett, M.K., Sack, L., Baraloto, C., Engel, J., Joetzer, E., Chave, J., 2015. Drought tolerance as predicted by leaf water potential at turgor loss point varies strongly across species within an Amazonian forest. *Funct. Ecol.* 29, 1268–1277.
- Nardini, A., Luglio, J., 2014. Leaf hydraulic capacity and drought vulnerability: possible trade-offs and correlations with climate across three major biomes. *Funct. Ecol.* 28, 810–818.
- Nardini, A., Pedà, G., Rocca, N.L., 2012. Trade-offs between leaf hydraulic capacity and drought vulnerability: morpho-anatomical bases, carbon costs and ecological consequences. *New Phytol.* 196, 788–798.
- Petrzellis, F., Nardini, A., Savi, T., Tonet, V., Castello, M., Bacaro, G., 2018. Less safety for more efficiency: water relations and hydraulics of the invasive tree *Ailanthus altissima* (Mill.) Swingle compared with native *Fraxinus ornus* L. *Tree Physiol.* 39, 76–87.

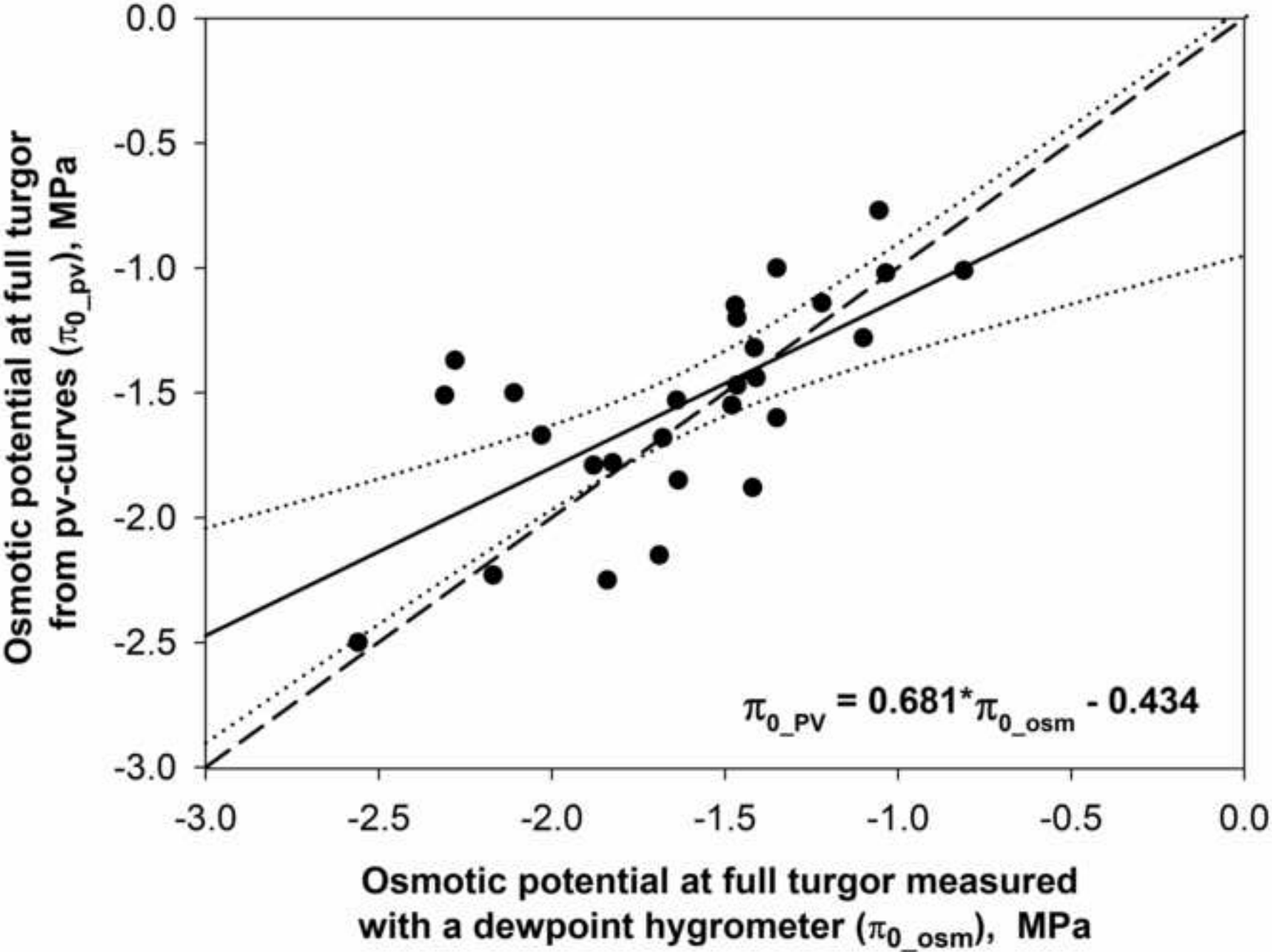
- Petruzzellis, F., Palandrani, C., Savi, T., Alberti, R., Nardini, A., Bacaro, G., 2017. Sampling intraspecific variability in leaf functional traits: Practical suggestions to maximize collected information. *Ecol. Evol.* 7, 11236–11245.
- Savi, T., Marin, M., Luglio, J., Petruzzellis, F., Mayr, S., Nardini, A., 2016a. Leaf hydraulic vulnerability protects stem functionality under drought stress in *Salvia officinalis*. *Funct. Plant. Biol.* 43, 370–379.
- Savi, T., Casolo, V., Luglio, J., Bertuzzi, S., Trifilo', P., Lo Gullo, M.A., Nardini, A., 2016b. Species-specific reversal of stem xylem embolism after a prolonged drought correlates to endpoint concentration of soluble sugars. *Plant Physiol. Bioch.* 106, 198–207.
- Savi, T., Dal Borgo, A., Love, V.L., Andri, S., Tretiach, M., Nardini, A., 2016c. Drought versus heat: What's the major constraint on Mediterranean green roof plants? *Sci. Total Environ.* 566–567, 753–760.
- Savi, T., Love V.L., Borgo A.D., Martellos S., Nardini A., 2017. Morpho-anatomical and physiological traits in saplings of drought-tolerant Mediterranean woody species. *Trees* 31, 1137–1148.
- Schneider, C.A., Rasband, W.S., Eliceiri, K.W., 2012. NIH Image to ImageJ: 25 years of image analysis. *Nat. Methods* 9, 671–675.
- Tognetti, R., Raschi, A., Jones, M.B., 2000. Seasonal patterns of tissue water relations in three Mediterranean shrubs co-occurring at a natural CO₂ spring. *Plant Cell Environ.* 23, 1341–1351.
- Trifiló, P., Raimondo, F., Savi, T., Lo Gullo, M.A., Nardini, A., 2016. The contribution of vascular and extra-vascular water pathways to drought-induced decline of leaf hydraulic conductance. *J. Exp. Bot.* 67, 5029–5039.
- Tyree, M.T., Hammel, H.T., 1972. The Measurement of the Turgor Pressure and the Water Relations of Plants by the Pressure-bomb Technique. *J. Exp. Bot.* 23, 267–282.
- Violle, C., Navas, M.-L., Vile, D., Kazakou, E., Fortunel, C., Hummel, I., Garnier, E., 2007. Let the concept of trait be functional! *Oikos* 116, 882–892.
- Wright, I.J., Reich, P.B., Westoby, M., Ackerly, D.D., Baruch, Z., Bongers, F., Cavender-Bares, J., Chapin, T., Cornelissen, J.H., Diemer, M., 2004. The worldwide leaf economics spectrum. *Nature* 428, 821–827.

475 Zhu, S.-D., Chen, Y.-J., Ye, Q., He, P.-C., Liu, H., Li, R.-H., Fu, P.-L., Jiang, G.-F.,
476 Cao, K.-F., 2018. Leaf turgor loss point is correlated with drought tolerance
477 and leaf carbon economics traits. *Tree Physiol.* 38, 658–663.

CONTRIBUTIONS:

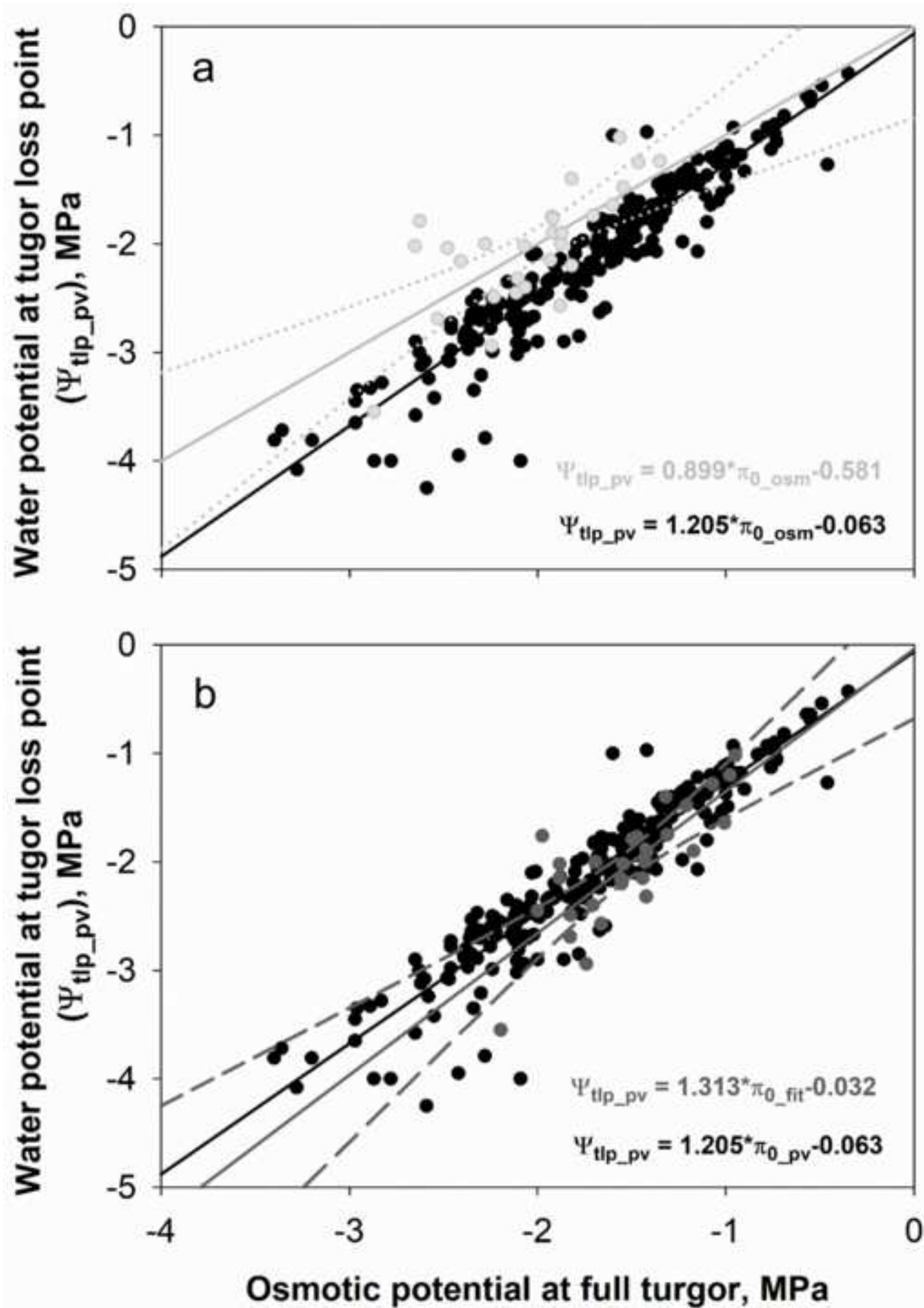
FP, TS and AN conceived and designed the study; FP and TS collected the data; FP, GB and AN analysed the data; FP, GB and AN wrote the manuscript, with the contribution of all authors.

Figure
[Click here to download high resolution image](#)



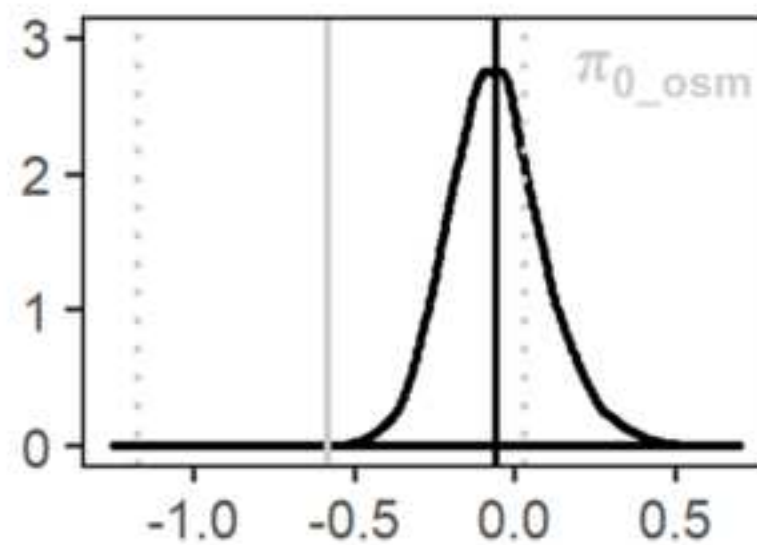
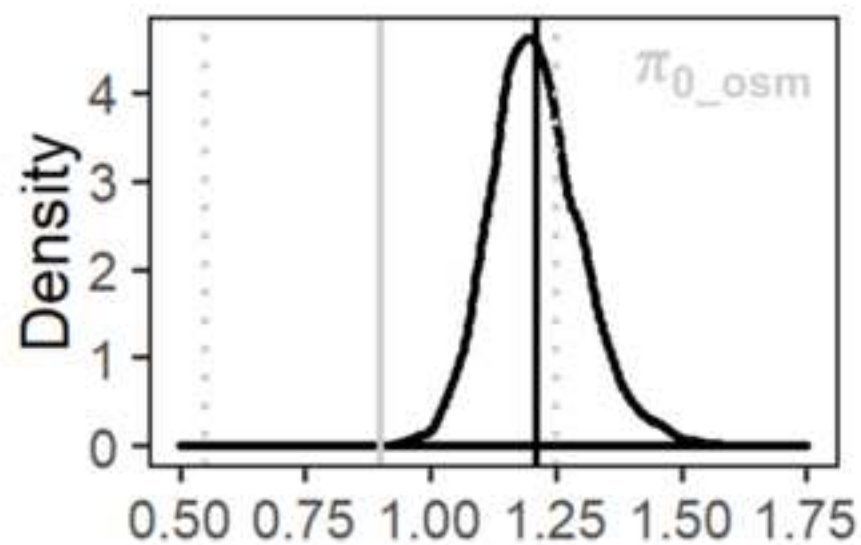
Figure

[Click here to download high resolution image](#)

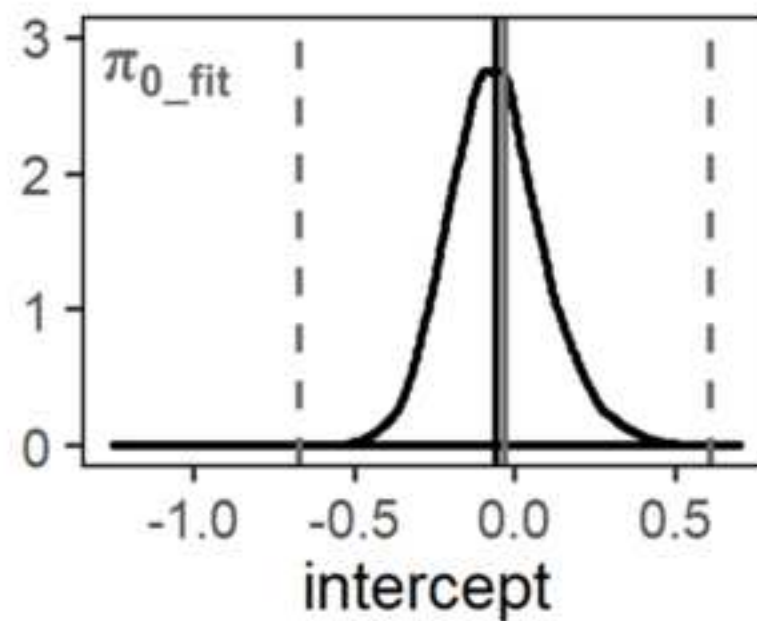
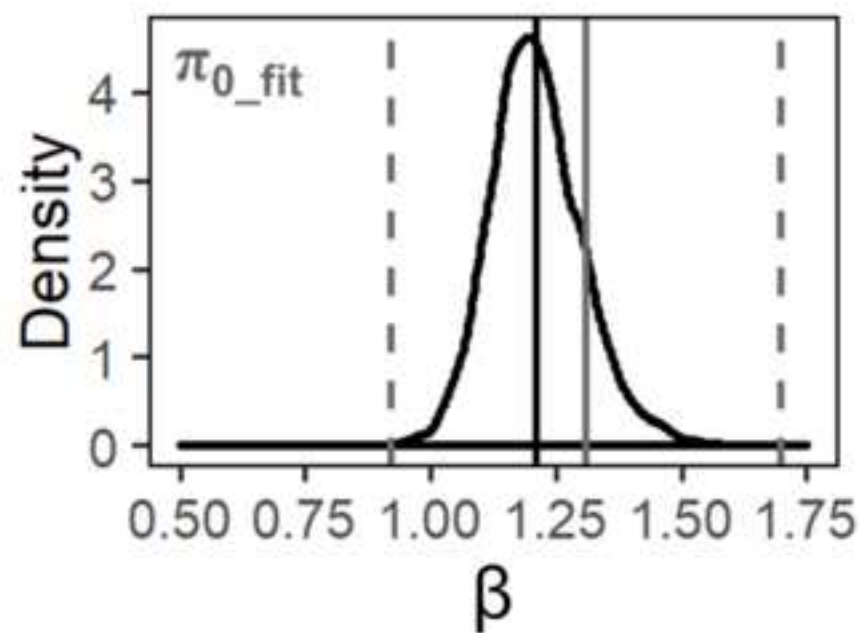


Figure

[Click here to download high resolution image](#)



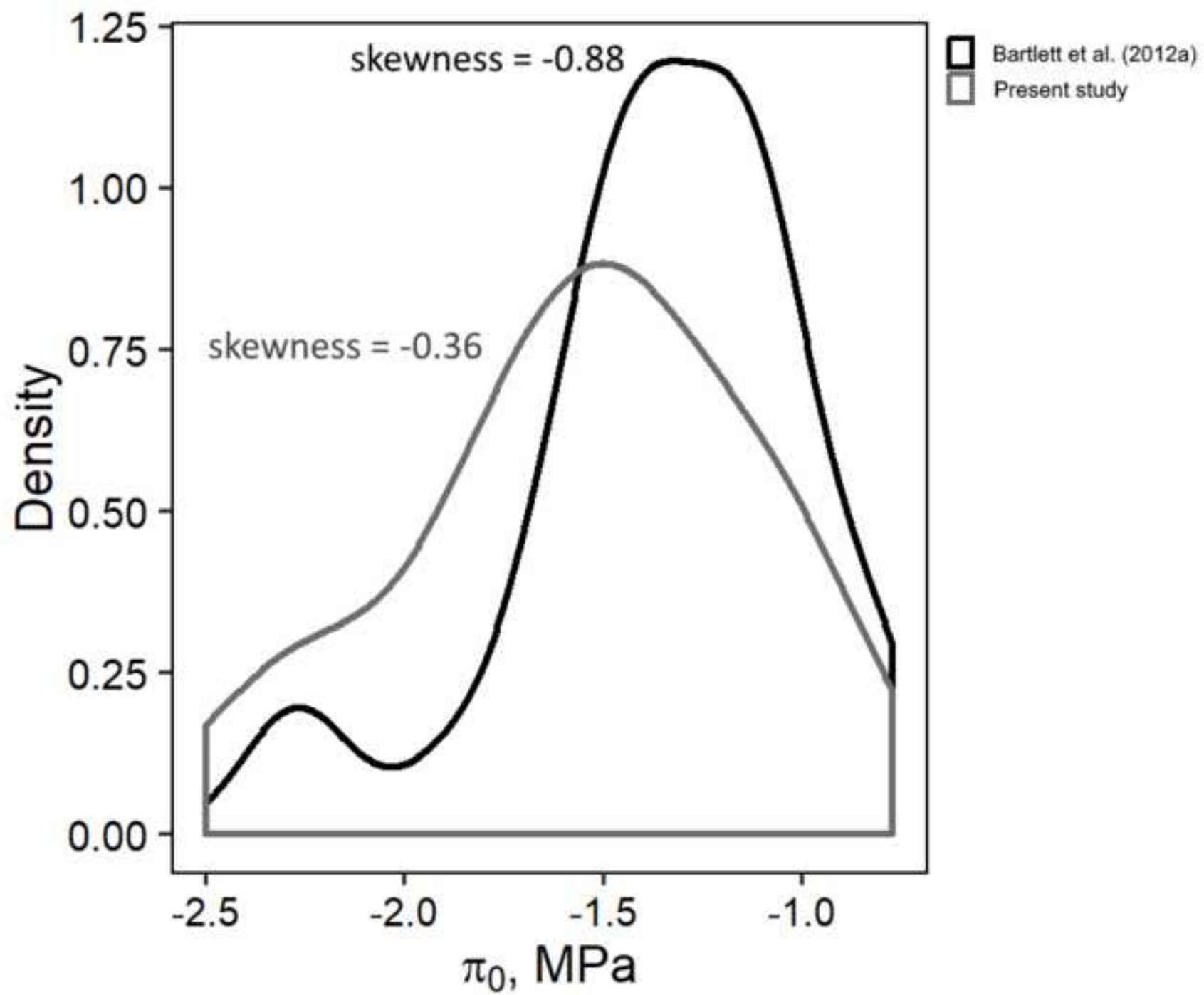
a)



b)

Figure

[Click here to download high resolution image](#)



Supplementary material
[Click here to download Supplementary material: TabS1.xlsx](#)

Supplementary material

[Click here to download Supplementary material: Supplementary_PPB_rev.docx](#)